#18

TEMPERATURE AND RADIATION OF LARGE METHANE/AIR JET FLAMES WITH WATER SUPPRESSION

J. P. Gore,
University of Maryland, College Park, MD 20770

D. D. Evans,
National Institute of Standards and Technology, Gaithersburg, MD 20899

B. J. McCaffrey,
University of Maryland, Baltimore, MD 21228

Radiation and extinction of large turbulent jet flames is of interest in the evaluation of hazard to personnel resulting from oil and gas well blowouts. Motivated by this problem, experiments concerning the feasibility of extinguishment of large (100-200 MW) and medium (1-10 MW) scale methane/air flames using water-sprays have been conducted in the past [1,2]. Measurements and predictions of flame structure and radiation properties of laboratory scale methane/air flames (ca. 20 KW) without water-suppression have also been reported [3-5]. Predictions of temperature and radiative heat fluxes for large (100-200 MW) flames without water-suppression also yielded encouraging results [5]. The objectives of the study reported here were: (1) to utilize data from reference 2 for medium (1-10 MW) scale flames to evaluate the effectiveness of analysis, and (2) to extend the analysis to treat the effects of liquid water suppressant on flame structure and radiation. In the following, the experimental methods are described briefly followed by a summary of the theoretical treatment. Results for flames without the addition of liquid water are described next. The paper concludes with a discussion of the effects of water addition on flame structure and radiation.

Methane was directed vertically upward from the floor of a 5 m deep underground pit. Air entered the pit from large openings at the surface. The fuel pipe was 104 mm in diameter and had a sudden contraction to 32 mm at the exit. Water was sprayed into the fuel stream using a pneumatic atomizing nozzle located 59 mm upstream of the pipe exit. A small fraction of the total methane flow was used for atomization. Water and atomizing methane were metered using rotometers. The main methane flow was measured using a laminar flow element. Six chromel-alumel thermocouple junctions formed from 0.5 mm wires were used to measure temperatures along the flame axis. Radiative heat fluxes to two representative locations around the flames (see inset of Fig. 2) were monitored using wide angle radiometers. All the flames considered here were turbulent (Re - 30,000 to 500,000) and had some effects of buoyancy (Ri - 0.000014 to 0.00012) as per the criterion of reference 6. Many of the flames were lifted from the burner exit.

Theoretical methods for flames without the addition of water were identical to those of Jeng et al. [3]. For flames with water added to the fuel stream, the locally homogeneous flow (LHF) approximation described in ref. [7] was used. Within this approximation, it was assumed that the transport of mass, momentum, and energy between the liquid water and the surrounding gases is much faster than the mixing between the jet and the ambient fluids. Based on past experimental findings [8], it was assumed that the addition of liquid water produced only thermal effects. These were treated

by modifying the state relationships for all scalar properties as a function of mixture fraction. The structure calculations were completed using a Favre-averaged K-ϵ-g model similar to past practice using the GENMIX algorithm [9]. Although, many of the flames were lifted from the burner, the effects of liftoff were neglected due to considerable uncertainties in the current understanding [10]. The radiation calculations were performed using the RADCAL algorithm [11] and the discrete transfer method [12].

Measurements(represented by symbols showing the best fit to the data from ref.[2] and not actual data points) and predictions of temperature along the axis of a 4.6 MW flame without water addition are shown in Figure 1. The measurements have not been corrected for the effects of radiation (expected to be ca. 200 K in the hottest portions). In regions near the burner exit the predictions mimic the data. This may be fortuitous in view of the lack of radiation corrections. In regions away from the burner, the measurements are ca. 400 K lower than the predictions. In addition to the uncertainities of the analysis(due to assumed initial conditions and neglect of the effects of liftoff), the discrepancies are caused by thermocouple radiation errors and flame-flapping in regions away from the injector exit.

Figure 2 shows measurements and predictions of total heat fluxes incident upon two detectors (for positions indicated in the inset) as a function of heat release rate. The shape, size, and position of the flame relative to the detectors change due to the effects of buoyancy [6]. The data show that the heat flux to both detectors increases rapidly with heat release rate in the 0.5 to 2.5 MW range, and then, due to the changing shape and size of the flame relative to the detector positions, the rate of increase is reduced considerably before increasing again at ca. 4.5 MW. It is encouraging to note that the analysis mimics this behavior. The magnitude of the radiative heat flux is under-predicted similar to past findings [3-5]. Past work [3] suggests that this is is due to the neglect to the turbulence radiation interactions. Based on the small differences in the predictions (which completely neglect radiation from soot) and measurements, it can be concluded that soot-radiation is a minor fraction of the total rediation for methane/air flames. This is also confirmed by earlier spectral intensity measurements [3,5], which indicated that molecular radiation was dominant. The agreement between measurements and predictions of radiative heat fluxes is much better than those of temperatures. Part of this is due to the integral nature of radiative heat flux, resulting in cancellation of errors in the detailed scalar distributions. Based on the encouraging predictions for flames without water-addition, the analysis was extended to treat the effects of water added to the fuel.

Figure 3 shows the state relationships for flames with water added to the fuel stream. Temperature, mole fraction of liquid water, mole fraction of water vapor, and mole fraction of carbon dioxide are plotted as a function of fuel equivalence ratio. Liquid water is present on the fuel-rich side of all the flames with water addition and holds the temperature at the equilibrium value corresponding to the partial pressure of water vapor. Once all the water is evaporated, the temperature rises rapidly, but its peak is lower due to the heat of vaporization and sensible heating of the water. Mole fractions of gases like carbon dioxide are reduced as shown in Figure 3 while mole fractions of water vapor are increased, resulting in non-trivial effects on absorption coefficients. As seen from the state relationships in Figure 3,

the present analysis implies that all the liquid water is evaporated within the flame. In practice, due to poor atomization particularly at large water-loadings, water penetrates into the fuel-lean regions and also gets ejected from the flame. This is expected to affect the temperature and radiation predictions for flames with water.

Measurements and prediction of peak temperatures along the axis of 4.6 MW flames as a function of nondimensional water mass flow rate are plotted in Figure 4. For a fixed methane flow (fixed heat-release rate), the location of the peak temperature (both measured and predicted) remains almost independent of the water flow rate due to the effects of increased momentum of the jet. As expected both data and predictions show a reduction in the peak temperature with increasing water-addition. Discrepancies between data and predictions for zero water-loading have been discussed above. As water-loading is increased, the differences between data and predictions are seen to decrease. This is not only because of the reductions in radiation corrections but also because of the assumption of complete water-evaporation. It is therefore expected that the radiative heat fluxes for flames with large quantities of water will be under-predicted by the analysis. Figure 5 shows measurements and predictions of radiative heat flux to a representative detector (normalized by the flux with zero water-loading) as a function of non-dimensional water flow-rate. As expected, the predictions under-estimate the heat flux for high water-loadings. Separated flow analysis, which takes into account the finite rates of mass, momentum and energy transfer between the liquid and gas phases, will be necessary for treating flames with the high water-loadings which are required for extinction.

ACKNOWLEDGEMENT This work is supported by the Mineral Management Service, Department of the Interior and the National Institute of Standards and Technology, Department of Commerce.

REFERENCES:

[1] Evans, D. and Pfenning, D., Oil and Gas J., **83** (17), 80, 1985.
[2] McCaffrey, B. J., "Momentum Diffusion Flame Characteristics and the Effects of Water Spray," NBSIR 86-3442., NIST, Gaithersburg, MD, 20899, 1986.
[3] Jeng, S. M., Lai, M. C., and Faeth, G. M., Combust. Sci. and Tech., **40**, 41. 1984.
[4] Jeng, S. M. and Faeth, G. M., J. Heat Trans. **106**, 891, 1984.
[5] Gore, J. P., Faeth, G. M., Evans, D. and Pfenning, D., Fire and Materials **10**, 161, 1986.
[6] Becker, H. and Liang D., Comb. Flame, **32**, 115, 1978.
[7] Faeth, G. M., prog. Energy Combust. Sci., **9**, 1, 1983.
[8] Seshadri, K, Comb. Flame, **33**, 197, 1978.
[9] Spalding, D. B., GENMIX: A General Computer Program for Two-Dimensional Parabolic Phenomena, Pergamon, Oxford, 1977.
[10] Pitts, W., 1988, "Assesment of Theories for the Behavior and Blowout of Lifted Turbulent Jet Diffusion Flames," Twenty-Second Symposium (International) on Combustion, The Combustion Institute, Pittsburgh, in press, 1988.
[11] Grosshandler, W., Int. J. Heat Mass Transfer **23**, 1447, 1980.
[12] Lockwood, F. C. and Shah, N. B., Eighteenth Symposium (International) on Combustion, The Combustion Institute, Pittsburgh, Pa, 1405, 1981.

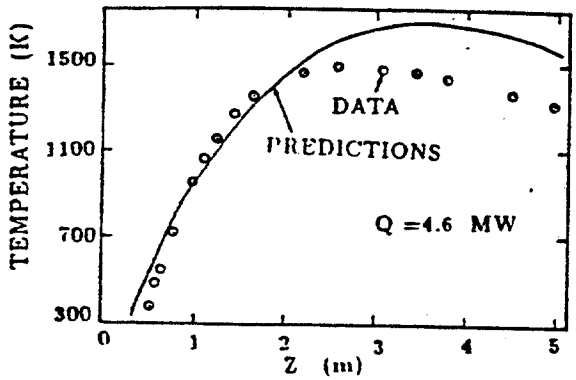

Fig. 1 Temperature along Flame Axis

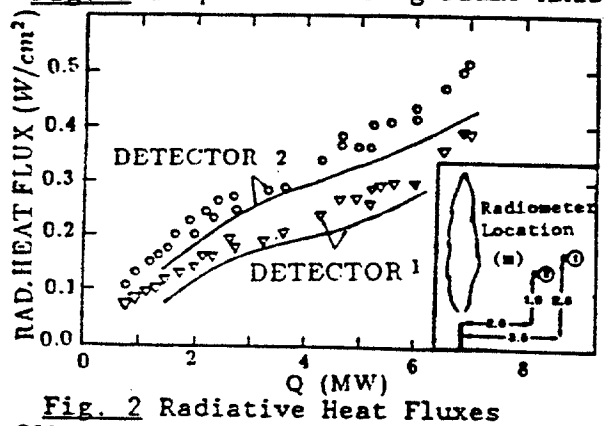

Fig. 2 Radiative Heat Fluxes

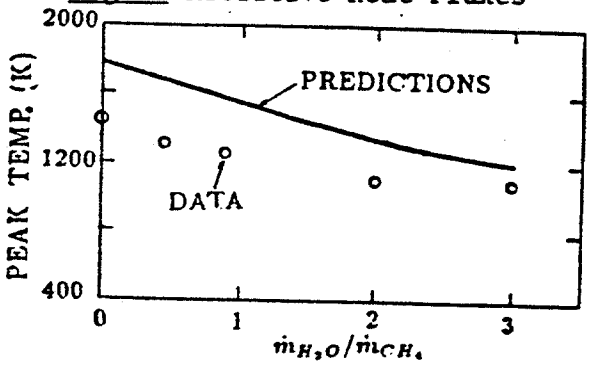

Fig. 4 Peak Temperatures with H_2O

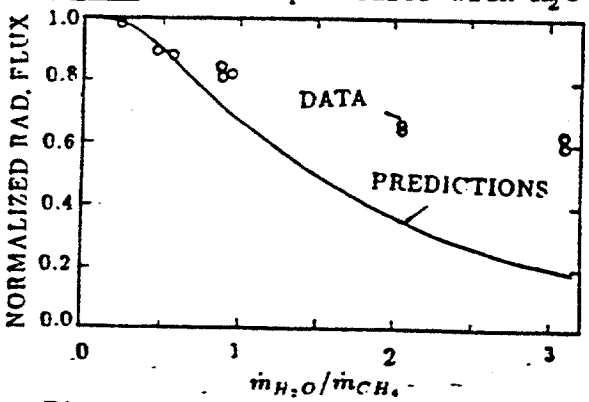

Fig. 5 Radiative Heat Fluxes with H_2O

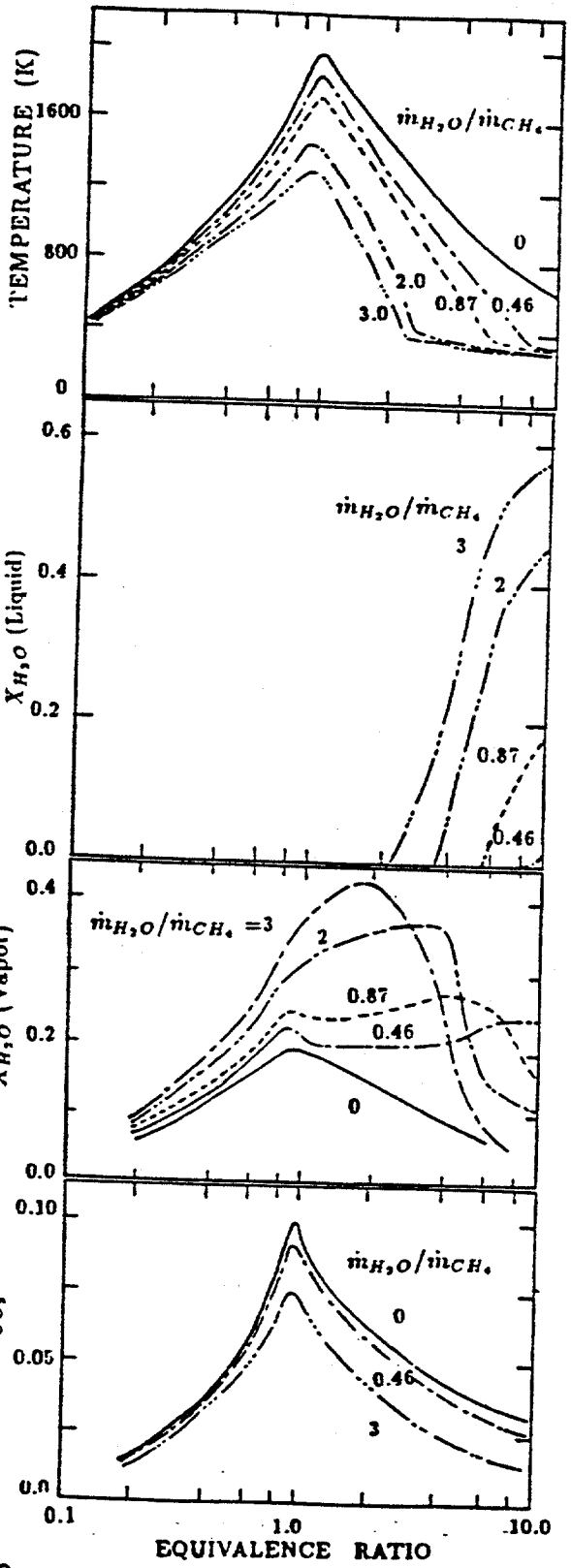

Fig. 3 State Relationships with H_2O